Micronetworks by End-Linking of Polystyrene. 1. Synthesis and Characterization by Light and Neutron Scattering

Markus Antonietti, Dietmar Ehlich, Karl J. Fölsch, and Hans Sillescu*

Institut für Physikalische Chemie der Universität Mainz, Jakob Welder Weg 15, D-6500 Mainz, West Germany

Manfred Schmidt

Max Planck Institut für Polymerforschung Mainz, Jakob Welder Weg 13, D-6500 Mainz, West Germany

Peter Lindner

Institut Laue-Langevin, Avenue des Martyrs, 156 X-38042 Grenoble Cedex, France.
Received August 2, 1988; Revised Manuscript Received November 12, 1988

ABSTRACT: Polystyrene (PS) chains with two reactive end groups prepared by anionic polymerization were terminated with a tetrafunctional cross-linking agent in tetrahydropyran solutions at concentrations low enough to obtain no macroscopic gelation. The resulting products, so-called μ-networks, were fractionated, yielding samples of molecular weights M_w between 100 000 and several millions g/mol and "apparent" polydispersity ratios M_w/M_n of 1.2–1.8. The lengths of the parent chains were varied between 20 and 140 monomer units. The μ-networks were characterized in toluene and cyclohexane solutions (good and Θ solvent, respectively) by viscosimetry and static and dynamic light scattering. Compared with linear polystyrene, all properties indicate the strong reduction of the molecular size of the μ-networks. The internal structure of the μ-networks was investigated by small-angle neutron scattering in toluene and cyclohexane solutions as well as in bulk matrices of linear and μ-network PS. The wave vector (Q) dependence of the scattering functions was approximated by power laws with distinct exponents, which can be used to define a fractal dimension d_f for these structures. The obtained d_f values are in good agreement with a theory made for networks close to the gel point. The μ-networks form a relatively open structure with many internal loops. They are freely interpenetrated by chains in the linear PS matrix and largely compressed in the μ-network matrices, where interpenetration is impeded.

I. Introduction

In recent years, much attention has been focused on the relationship between structure and dynamic properties of polymer networks. The obvious way to resolve this problem is to prepare elastomeric networks with well-defined topological or structural parameters, so called "model" networks, and to characterize the dynamics by variation of the available "chemical" parameters. Usually, narrowly distributed telechelic chains are cross-linked at both ends with a stoichiometric amount of cross-linking agent with a well-defined functionality f.

This kind of procedure is described in publications and extensive reviews (see for instance refs 1–6) and should not be the essential subject of our discussion. However, these systems behave not as ideal as expected; they contain always a varying amount of certain defect structures (ref 7). In addition, they are very difficult to purify or to handle. Also, the usual methods of polymer analysis, for instance light scattering, are not applicable in the bulk state. Thus, swelling experiments or neutron scattering are the predominant methods for investigating network structure properties.[1]

In the present paper we wish to follow a different course: we demonstrate the advantages of synthesizing well-defined microgel–network particles with dimensions in the nanometer range as models for macroscopic structures. These μ-networks are more easy to handle, to purify and to adjust to a given instrumental geometry. Also, one can readily determine the solution properties of these structures; therefore, one should have access to a better understanding of the network topology.

In our previous work[8] we have investigated polystyrene (PS) μ-gels prepared by intramolecular cross-linking of linear PS in dilute solutions. However, we were confronted with the still puzzling result that many structural and dynamical properties of these μ-gels show surprisingly small changes in comparison with linear PS even for large cross-linking densities with an average number of only 10 monomer units between cross-links. The assumption of a quasi-linear arrangement of many small rings along the chain can explain some results but leaves too many open questions.[8]

In the present paper, we wish to describe the synthesis of end-linked μ-networks prepared by a special anionic polymerization technique and characterized by GPC, static and dynamic light scattering, and viscosity measurements in solution. Small-angle neutron-scattering experiments (SANS) in solution and in the bulk state complete the structure information for smaller distances. In our following paper,[9] the following paper in this issue, we shall report dynamic mechanical and polymer diffusion experiments, which are then related with the structure properties.

II. General Considerations

In pure polymer materials, the condensation of α,ω-telechelic polymers results in macroscopic networks.[2-4] Reducing the polymer volume fraction Φ_P during the cross-linking reaction increases the number of small cyclic structures (complete conversion is always assumed). In the limit of infinite dilution, only the elementary structures are formed. Figure 1 sketches these smallest units for termination agents with the functionality f = 2, 3, and 4. The special case of ring polymers is already well examined[10,11] and attracts the attention of rheologists because of the very special restriction of molecular mobility by the geometrical structure.

In the intermediate range of concentrations, one should expect the continuous transition between the elementary structure and the macroscopic network: the amount of higher condensation products increases with increasing concentration until the gel point is reached. This behavior is qualitatively sketched in Figure 2, where the probability of formation H for the different species is plotted over Φ_P.

0024-9297/89/2222-2802$01.50/0

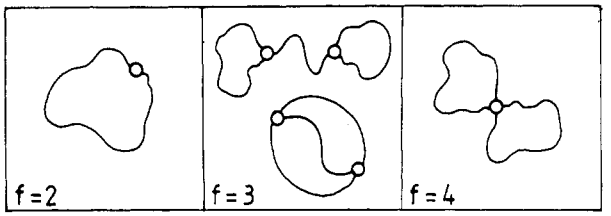

Figure 1. Elementary structures of cyclic polycondensation reactions for cross-linking agents with functionalities f = 2–4.

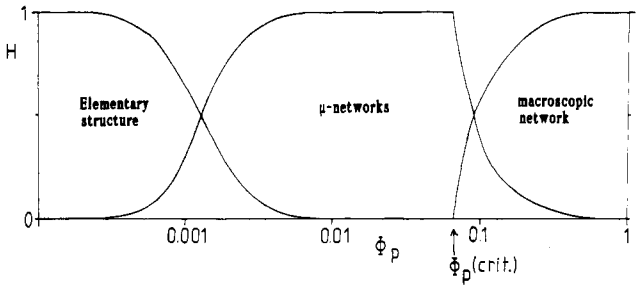

Figure 2. Probability of formation, H, of different structures in dependence of the volume fractions of polymer, Φ_P, during the cross-linking reaction. Below a critical value Φ_P(crit) no macroscopic gel is formed, but μ-networks are formed. At very low concentrations the elementary structure should be obtained.

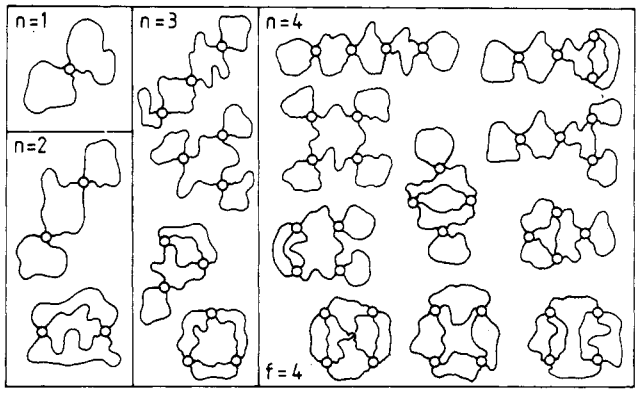

Figure 3. First four orders (number of cross-linking centers, n = 1–4) of μ-networks with f = 4.

The critical volume fraction of gelation Φ_P(crit) depends on f and the length of the parent polymer. It cannot be predicted in a straightforward way by using the classical gelation[7] or cascade theories,[12] because the internal cyclization, the predominant effect, is not taken into account.

The higher condensates or μ-networks formed in the intermediate concentration regime are also present in the products which are made beyond the gel point. In this case they are simply called "sol fraction". The diversity of possible geometrical structures can be taken from textbooks of graph theory[13] and is shown in Figure 3 for f = 4, where n is the number of cross-linking centers (a type of degree of polycondensation). A similar picture is already shown in ref 15. Note that the conversion is always complete and that the topological degeneracy becomes large even at small n. To obtain structures with a maximal size, the μ-networks described here are made just below the critical volume fraction Φ_P(crit). Intracatenation causes more complex structures (for instance "olympic" gels, see ref 39), which are omitted in Figure 3.

In the context of macromolecular branching, we may follow the opinion[16] that theory is much more advanced than experiments and try to improve the experimental situation. Therefore, we measure averaged properties of these structures and compare them with linear chains. A consistent relation of the results with static and dynamic properties of continuous networks is probably outside the range of this first set of experiments: all results should be extrapolated to $M \rightarrow \infty$ and $\Phi_P \rightarrow 1$. However, our results may contribute to a better understanding of network defects. In particular, our system contains loops of equal size that are not properly included in present network theories although they should be more frequent than dangling ends in "real" networks, where loops are formed in pregel intracatenary reactions[17] and remain in the final product.

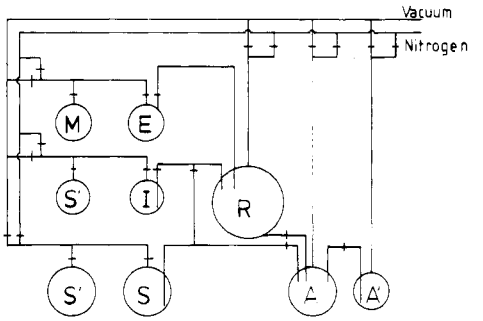

Figure 4. Setup for anionic polymerization and subsequent polycondensation.

III. Experimental Section

1. Polymer Synthesis. As mentioned above, most of the model networks are made in a two-step procedure: synthesis of narrowly distributed bifunctional telechelic linear chains and condensation with stoichiometric amounts of polyfunctional termination agents.

For the first step, the anionic polymerization of styrene is known to fulfill all demands; with sodium dihydronaphthylide as initiator, one readily obtains α,ω-telechelic polymers. Because of the sterical hindrance and the small diffusion coefficients of polymers in a viscous medium, the second step is very slow, and the stoichiometric end of reaction is possibly never reached. Therefore, we decided to apply a very fast ionic reaction, namely, the substitution of chlorine at silicon by carbanions in a polar solvent: This

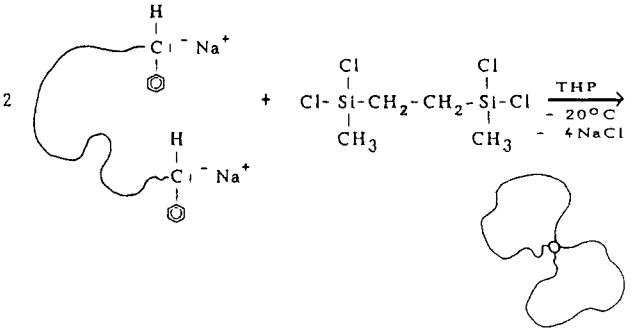

reaction is well-known for the synthesis of star polymers (see, for instance, ref 18); it is practically free from side reactions by ion transfer and results in topologically well-defined products.

It is absolutely necessary for the aimed products to have bifunctional polymers in amounts near 100% and also to balance carefully the stoichiometry at equality. We achieved this with a special construction mainly based on the addition of all important reactants through the gas phase. Figure 4 sketches this all-glass setup. Vacuum or high-purity nitrogen can be transferred to every subunit, which can be locked with PTFE valves. Let us briefly delineate the typical procedure for polymer synthesis.

Styrene (99%, Aldrich) and tetrahydropyrane (THP, 99%, Merck) are purified by the usual route, filled in, and degassed in flasks M and S, respectively. Bis(dichloromethylsilyl)ethane as a termination agent (for the synthesis, see ref 18) is filled into A and is degassed 3 times by melting and freezing the product, pulling a vacuum in every cycle at −30 °C. Sodium dihydronaphthylide is synthesized following standard reactions[19] in I. The reaction is carried out in the stirring reactor R. The correct amount of initiator is transferred from I to R and is filled up with

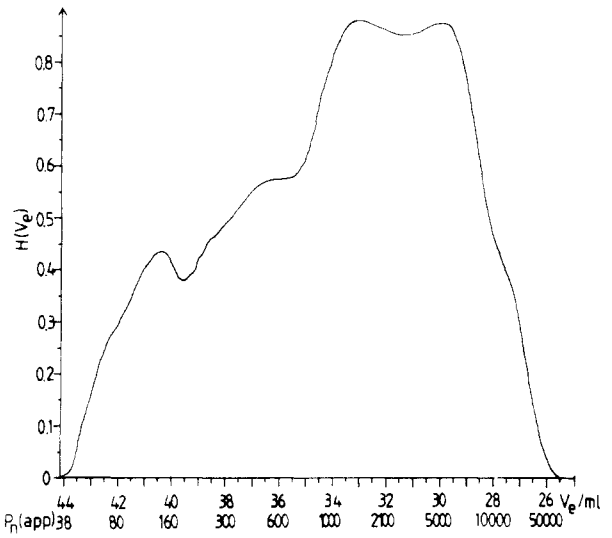

Figure 5. GPC curve of the crude product of the polycondensation reaction. The normalized detector signal H is plotted versus the elution volume. For illustration, apparent degrees of polymerization obtained from linear polymers are also given.

the solvent from S. The temperature is held at −50 to −40 °C.

The monomer is then transferred to the evaporation flask E where it is purified a last time with the solid lithium salt of fluorene. The following addition of the monomer to the initiator/solvent mixture is regulated only by the vapor pressure of styrene; by controlling the temperature at E, the speed of addition can be changed. This procedure is mainly based on a simpler setup, described in ref 20. Usual reaction times with our system are roughly 90 min. Because of the kinetic control and rapid stirring, one can obtain very narrowly distributed polymers. Furthermore, kinetic mixing problems in polar solvents are avoided. The functionality f' was checked to be larger than $f' \approx 1.98$.

The termination reaction with the multifunctional cross-linking agent was also carried out via the gas phase. Because of the small vapor pressures, one can titrate the "living" red solution to a nearly colorless finite state. Worth mentioning is the slow approach to equilibrium, which takes up to 5 h. The ratio of extinctions before the start and at the end of the termination reaction determines in a first approximation the amount of dangling ends. Since this ratio was typically larger than 500, and impurity termination can be neglected in comparison, we estimate the fraction of PS in dangling ends as <0.2%. A model reaction with monofunctional polymers yields four-arm stars in amounts of 70% the remains consisting essentially of three-arm stars (without fractionation). This corresponds to a cross-linking functionality $f = 3.7$ which we have to take into account for further examination. The lower functionality is in contrast to the data described in the literature,[18] where nearly complete linking was obtained. On one hand, this is caused by the relatively short reaction times applied during our experiments; on the other, the reaction speed is further decreased by the accurate balance of stoichiometry (during star synthesis it is advantageous to work with a surplus of reactive chains).

Typical degrees of polymerization of the linear precursor polymer are between 10 and 200 monomer units; this corresponds to critical polymer concentrations during the condensation reaction between 10% and 3%. Above these values macroscopic gelation occurs.

A typical GPC spectrum of a product is shown in Figure 5. From the above-mentioned oligomeric material up to very high molecular weight everything is enclosed. Decreasing the polymer concentration during the cross-linking reaction by a factor of 4 leads to an increase of the low molecular weight part, as checked in an additional experiment. In comparison to linear polycondensates, the elution peak is highly broadened. This may correspond to the formation of closed, fully reacted structures that are not accounted for in the theoretical description of polycondensation.[7] For all further experiments the samples are fractionated 3 times in methanol/tetrahydrofuran mixtures. The resulting fractions are listed in Table I.

Table I
Sample Designations and Apparent Degrees of Polymerization As Obtained by GPC

sample	P_N(app)	P_w(app)	P_w/P_N (app)	comments
Lin104	104	108	1.04	samples for
N2000/104	2050	2500	1.22	characterization in
N3600/104	3620	4560	1.26	solution
N4600/104	4620	8460	1.83	
N8900/104	8900	16500	1.85	
Lin39	39	42	1.08	
N1700/39	1740	2410	1.39	
Lin55	55	59	1.07	SANS measurements
N1000/55	990	1260	1.27	in solution
Lin66	66	69	1.05	
N4200/66	4210	5050	1.20	
Lin24	24	27	1.10	matrices for SANS
N800/24	788	945	1.20	measurements in
Lin71	71	75	1.05	bulk
N2900/71	2917	4431	1.51	
Lin1700	1680	1750	1.04	
Lin25	25	27	1.08	fully deuterated
N770/25	770	1010	1.31	SANS
N1200/25	1210	1670	1.38	measurements in
N1600/25	1610	2600	1.62	bulk
Lin37	37	39	1.05	fully deuterated
N800/37	800	870	1.09	SANS
N1000/37	1000	1120	1.12	measurements in
N1200/37	1220	1440	1.18	bulk
N1600/37	1570	2000	1.27	
Lin62	62	65	1.05	fully deuterated
N1000/62	1010	1120	1.11	SANS
N1300/62	1290	1460	1.13	measurements in
N1700/62	1700	2090	1.23	bulk
N2300/62	2300	3290	1.43	

We have also isolated the elementary structure, the eight-shaped polymer, by choosing a very low concentration during the condensation reaction; these results are published elsewhere.[21] Some of the fractions listed in Table I are fully deuterated (99.8% deuterium content) for performing neutron-scattering experiments in the bulk. In their synthesis it was crucial to use self-made styrene-d_8 (synthesis see ref 22) in order to achieve functionalities of the parent polymer which are comparable to those of the protonated species. Experiments with commercial deuterated monomer failed because of side reactions due to impurities which could not be removed.

2. Solution Viscosity Measurements. The viscosity measurements were performed in toluene at 20.0 °C and in cyclohexane at 34.5 °C with an automatic Schott AVS300 instrument (Ubbelohde viscosimeter) which allows the determination of the flow time with an accuracy of 0.01 s. The solutions were made by dissolving the samples in freshly distilled, sodium-dried toluene or cyclohexane. The flow times were determined for six to nine concentrations ranging from 12 to 2 g/L.

3. Static and Dynamic Light Scattering. Light-scattering experiments were carried out for four fractions in toluene at 20.0 °C and in cyclohexane at 34.5 °C. The spectrometer and procedure for simultaneous static and dynamic light scattering is extensively described in previous publications.[8,23] Most measurements were performed at the 647.1-nm line of a krypton ion laser (Spectra Physics). Some measurements were repeated with an argon ion laser (Spectra Physics 2020) working at 457.9 nm and gave essentially the same results. In cyclohexane, $\partial n/\partial c$ was determined with an Bodmann-Cantow refractometer at 647 nm as $\partial n/\partial c = 0.158$, whereas in toluene the extrapolated literature value yielded $\partial n/\partial c = 0.110$. In contrast to our earlier work,[8] we clarified the samples by filtering through 0.2-μm filters (Sartorius Co.). Because of possible concentration changes during the filtering procedure, the final concentrations were checked with a refractive index detector (toluene solutions) and with UV measurements (only cyclohexane solutions). In cyclohexane no loss of sample could be detected. In toluene, only the fraction with the highest molecular weight exhibited a lower concentration after filtering. Due to the low sensitivity of the RI detector, the concentration could not be determined accurately enough for a precise

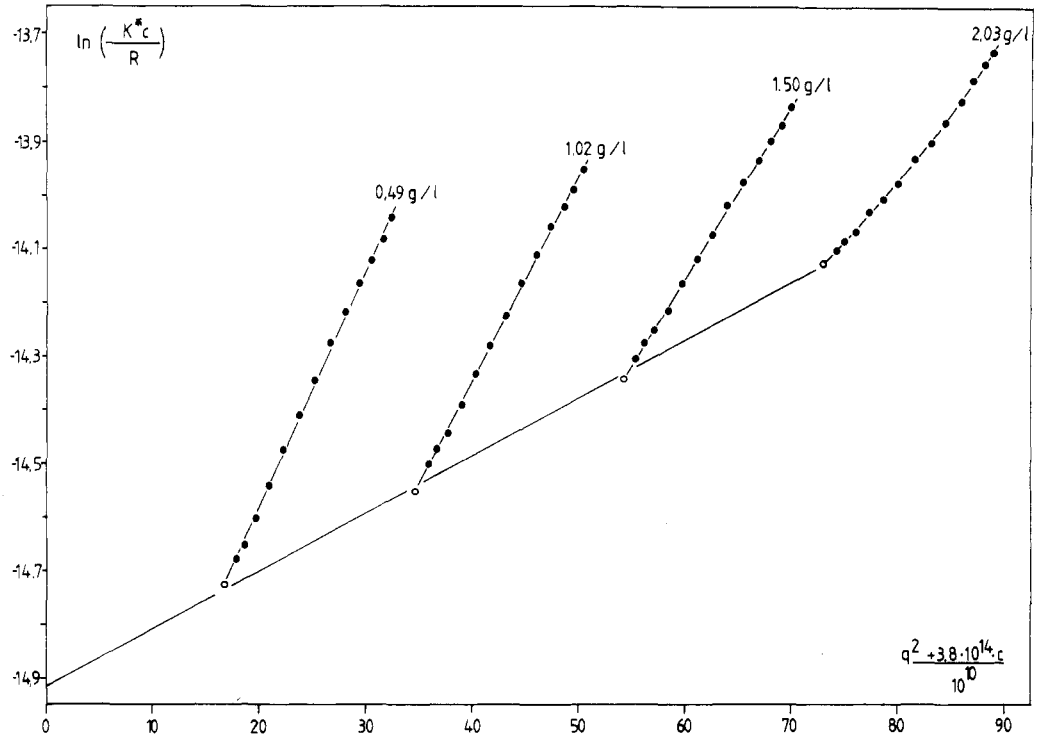

Figure 6. Guinier plot of the static light-scattering intensities for sample N4600/104 in toluene at 20 °C.

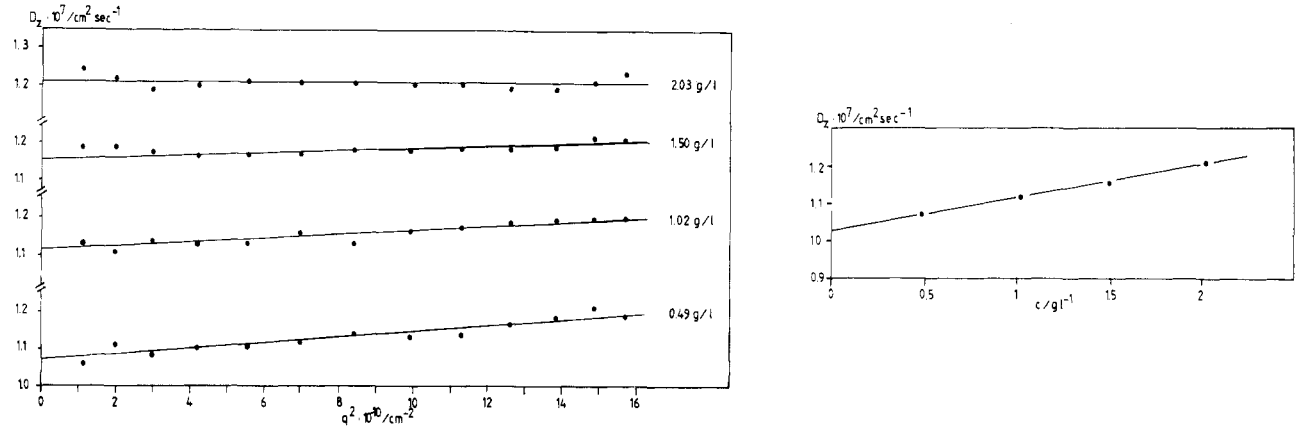

Figure 7. Angular and concentration dependence of the reduced first cumulant $D_z(q) = \Gamma/q^2$ as measured by dynamic light scattering for N4600/104 in toluene at 20 °C.

M_w determination. In this case we adopted the measured value in cyclohexane.

4. Small-Angle Neutron Scattering. The small-angle neutron-scattering experiments (SANS) were carried out at the Institut Laue-Langevin in Grenoble, France, using the small-angle diffractometers D11 and D17.[24] Measurements on D11 were performed by using sample-to-detector distances of 1.2, 2, 5, 10, and 20 m and an incident neutron wavelength of $\lambda = 0.6$ nm; measurements on D17 were carried out at the 1.4- and 3.45-m position with $\lambda = 1.2$ nm. The distribution of wavelength $\Delta\lambda/\lambda$ was 10%. The neutron counts on the two-dimensional detector were radially averaged, normalized to the incoming neutron dose, and corrected for transmission and sample volume. The incoherent scattering of water was taken as a calibration for absolute scattering intensity and to correct for detector inhomogeneities.

SANS experiments in solution were carried out in optical cuvettes (boron-poor Suprasil from Hellma Co.) with path lengths of 1, 2, and 5 mm. Protonated μ-networks in deuterated toluene or cyclohexane (99.5% both, Aldrich) were prepared in a 2% solution as mentioned above. During the measurements the temperature was held at $T = 20$ °C (toluene) or 34.5 °C (cyclohexane).

In the SANS experiments in the bulk we took deuterated polymers as a probe (also 2%) in protonated polymeric material; in addition to the behavior of μ-networks in a matrix of linear macromolecules, we examined melts of pure μ-network material. The usage of protonated polymers as a matrix strongly increases the influence of incoherent scattering but minimizes the disturbance of scattering from protonated cross-linkers and voids at small values of the scattering vector Q. The polymers were mixed in solution, precipitated, and dried as already described.[25] In order to achieve an optically clear pellet for minimizing excess scattering, we tempered the samples at 150 °C for half an hour and applied a pressure of 10 kbar at this temperature. As a sample holder we used our cell constructed for light-scattering experiments on polymer films[25] modified for pellets with 13-mm diameter and 1-mm thickness. The so-produced samples are nearly free from excess scattering and allow measurements in the glassy state at 20 °C.

All measurements were corrected for the scattering of the "solvents" by subtraction of the independently measured values of the pure matrices.

IV. Results and Discussion

1. Viscosity and Light Scattering. For the samples N2000/104 through N8900/104 (see Table I) we have determined the absolute molecular weight, the hydrodynamic radius, and the radius of gyration within one series of fractions. For illustration, the static and dynamic

Table II
Characterization of μ-Networks

sample	N200/104	N3600/104	N4600/104	N8900/104
		Toluene		
$M_w/10^{-6}$ g·mol^{-1}	0.54	1.29	2.9	(6.2)
$\langle s^2\rangle_z^{0.5}$/nm	20.0	31.5	45.0	65.0
r_H/nm	16.6	23.3	35.3	52.3
$[\eta]$/cm^3·g^{-1}	55.1	75.4	111.3	141.2
r_η/nm	16.9	24.8	36.6	52.6
r_η/r_H	1.016	1.07	1.035	1.006
$A_2/10^{-4}$ cm^3·g^{-2}	1.82	1.20	0.91	0.24
k_D/cm^3·g^{-1}	50.2	74.8	103	149
k_H	0.47	0.57	0.57	0.69
		Cyclohexane		
$M_w/10^{-6}$ g·mol^{-1}	0.56	1.28	2.78	6.01
$\langle s^2\rangle_z^{0.5}$/nm	16.5	25.0	29.0	43.5
r_H/nm	13.2	18.7	25.5	37.3
$[\eta]$/cm^3·g^{-1}	32.7	42.2	51.4	55.0
r_η/nm	14.3	20.6	28.3	37.6
r_η/r_H	1.08	1.10	1.10	1.01

light-scattering measurements in toluene of sample N4600/104 are shown in Figures 6 and 7. The static scattering curves exhibit the expected shape for rather compact, spherical structures. Therefore we decided to take a logarithmic plot of K^*c/R over q^2 in order to describe the q dependence with straight lines. The radius of gyration is calculated by using the form factor of a sphere. The angular dependence of the diffusion coefficient is weak; the data can be easily extrapolated to $q \to 0$ and $c \to 0$ to obtain the hydrodynamic radius of the μ-network particles. Table II lists the results, including those of viscosity measurements in toluene and cyclohexane. It should be noted that the apparent molecular weights determined by GPC are much smaller than M_W determined by static light scattering.

The comparison of the intrinsic viscosities of the μ-networks with linear polystyrene molecules is shown in parts a (toluene) and b (cyclohexane) of Figure 8. The values of the linear polymers are taken from ref 26–29. Describing the data with simple scaling laws, which is surely a crude approximation, leads in toluene to

$$[\eta]_{\mu N} = 2.43 \times 10^{-1} M_w^{0.41\pm0.02} \quad [\eta] \text{ in cm}^3/\text{g} \qquad (1a)$$

$$[\eta]_{lin} = 1.07 \times 10^{-2} M_w^{0.724} \qquad (2a)$$

and in cyclohexane to

$$[\eta]_{\mu N} = 1.102 M_w^{0.26\pm0.05} \qquad (1b)$$

$$[\eta]_{lin} = 8.46 \times 10^{-2} M_w^{0.50} \qquad (2b)$$

Index a denotes measurements in toluene and b in cyclohexane (in the equation numbers). In the case of the cyclohexane (CH) measurements, the dependence has a significant curvature to a molecular weight independent intrinsic viscosity at higher M_w values. In all cases we observe that the μ-networks have a more compact structure compared to the linear chains. The dotted line in Figure 8a indicates the behavior of swollen spheres with a constant density, which is typically obtained for homogeneous network particles.[30] Calculating the Zimm–Kilb factor g'[31] results in

$$g' \equiv [\eta]_{\mu N}/[\eta]_{lin} \qquad (3)$$

$$\text{in toluene:} \quad g' = 22.7 \times M_w^{-0.31} \qquad (3a)$$

$$\text{in CH:} \quad g' = 13.0 \times M_w^{-0.24} \qquad (3b)$$

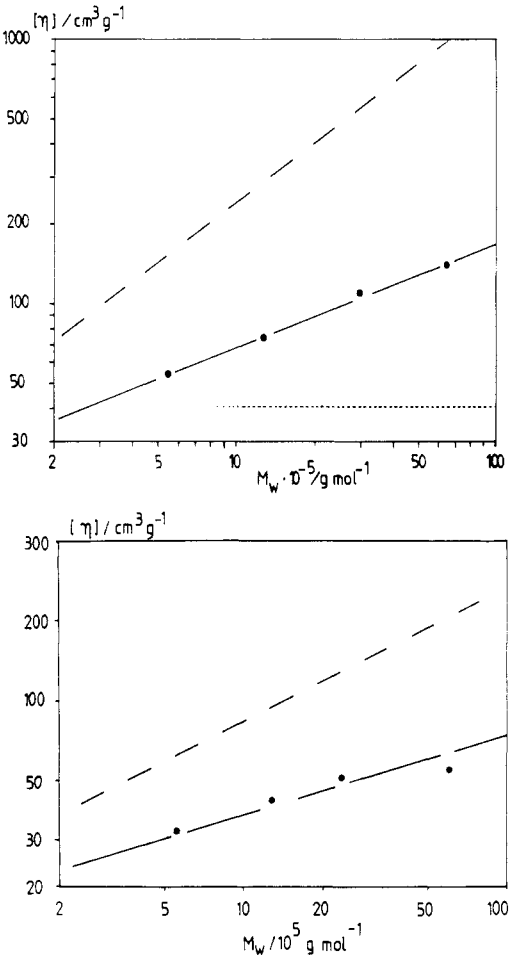

Figure 8. Intrinsic viscosities $[\eta]$ of the μ-networks N2000/104–N8900/104 in toluene at 20 °C (a, top) and cyclohexane at 34.5 °C (b, bottom). The dashed line indicates the behavior of linear polystyrene, the dotted line (toluene) the behavior of swollen spheres with a similar cross-linking density.

For both solvents g' is a function of the molecular weight. For the largest μ-networks (sample N8900/104), the hydrodynamic volume is contracted by a factor of 6 in toluene (factor of 4 in CH) as compared to linear chains of the same molecular weight. As mentioned above, it is also impossible to model the μ-networks as spheres with constant density, which would have a molecular weight independent intrinsic viscosity. If we compare the data with randomly branched polymers of similar cross-linking density made by copolymerization of styrene and 1,4-divinyl-2,3,5,6-tetrachlorobenzene,[32] we observe that the contraction factors reported here are higher than the referred ones. This can be explained by the strongly reduced amount of dangling ends according to different synthesis and topologies, thus supporting some of our structure assumptions.

We did not explicitly compare our results to the Zimm–Stockmayer theory for the hydrodynamic behavior of branched polymers[33] because it does not account for internal cyclization. In good agreement with our results, the authors of ref 32 obtain for the limit of high molecular weight a scaling exponent for the contraction factor g' of $g' \sim M_w^{0.30}$, which is within the experimental error of our experiments. Star polymers behave in a different way[34] and can be described by a constant g' factor, whereas combs show nearly the same hydrodynamic contraction as the randomly branched polymers (see also ref 34).

Figures 9a,b and 10a,b (a denotes measurements in toluene, b in cyclohexane) show the behavior of the hy-

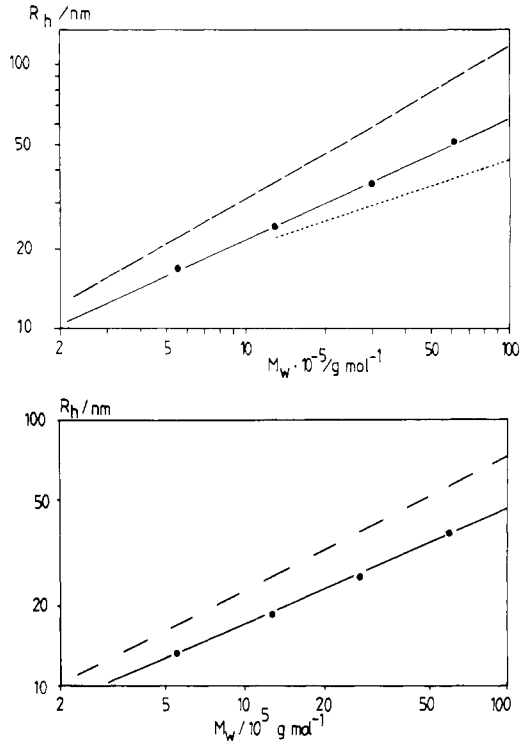

Figure 9. Hydrodynamic radii of the series N2000/104–N8900/104 as obtained from dynamic light scattering in toluene (a, top) and cyclohexane (b, bottom) (see Figure 8 caption).

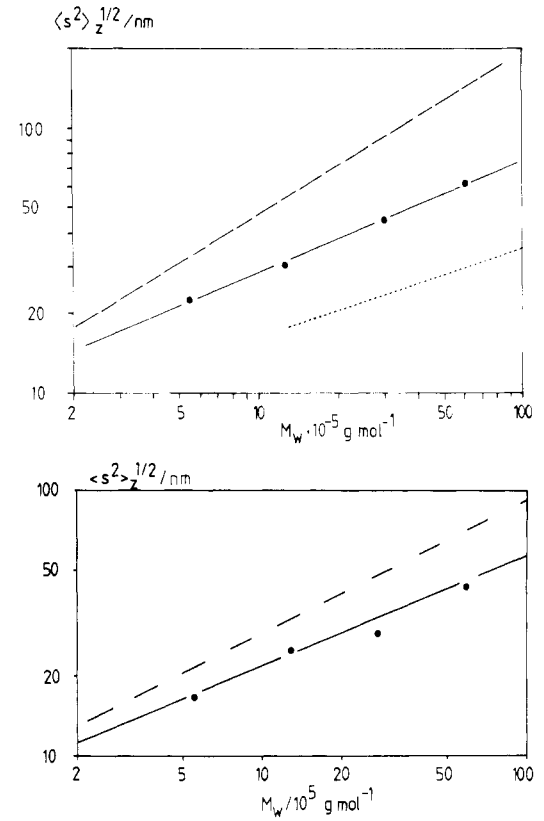

Figure 10. Radii of gyration of the series N2000/104–N8900/104 as obtained from static light scattering in toluene (a, top) and cyclohexane (b, bottom) (see Figure 8 caption).

drodynamic radius and of the radius of gyration of the μ-networks in comparison with the data of linear chains taken from the literature.[23,29] Again, the dotted lines represent the behavior of homogeneous swollen spheres. Also, by the different radii we observe a contraction of the

Table III
Contraction Ratios of μ-Networks in Solution

sample	N2000/104	N3600/104	N4600/104	N8900/104
		Toluene		
g'	0.364	0.265	0.224	0.154
$g^{0.5}$	0.613	0.570	0.510	0.442
h	0.757	0.676	0.623	0.568
$h/g^{0.5}$	1.23	1.19	1.22	1.29
		Cyclohexane		
g'	0.517	0.441	0.368	0.265
$g^{0.5}$	0.760	0.762	0.605	0.612
h	0.770	0.722	0.674	0.664
$h/g^{0.5}$	1.01	0.95	1.11	1.08

μ-networks compared to linear chains; all data can be approximately described by scaling laws.

in toluene:

$$\langle 1/r_H \rangle_z^{-1}(\mu N) = 3.18 \times 10^{-9} M_w^{0.47} \quad (4a)$$

$$\langle 1/r_H \rangle_z^{-1}(\text{lin}) = 1.08 \times 10^{-9} M_w^{0.58} \quad (5a)$$

$$\langle s^2 \rangle_z^{1/2}(\mu N) = 4.09 \times 10^{-9} M_w^{0.47} \quad (6a)$$

$$\langle s^2 \rangle_z^{1/2}(\text{lin}) = 1.11 \times 10^{-9} M_w^{0.61} \quad (7a)$$

in cyclohexane:

$$\langle 1/r_H \rangle_z^{-1}(\mu N) = 5.29 \times 10^{-9} M_w^{0.42} \quad (4b)$$

$$\langle 1/r_H \rangle_z^{-1}(\text{lin}) = 2.29 \times 10^{-9} M_w^{0.50} \quad (5b)$$

$$\langle s^2 \rangle_z^{1/2}(\mu N) = 6.64 \times 10^{-9} M_w^{0.42} \quad (6b)$$

$$\langle s^2 \rangle_z^{1/2}(\text{lin}) = 2.90 \times 10^{-9} M_w^{0.50} \quad (7b)$$

where the radii, r, are in meters. Defining the contraction factors of $\langle s^2 \rangle_z^{1/2}$ and r_H of internal cross-linking by the ratios $g^{0.5}$ and h, we obtain

$$g^{0.5}(\text{tol}) = 3.69 \times M_w^{-0.14} \quad (8a)$$

$$h(\text{tol}) = 2.94 \times M_w^{-0.11} \quad (9a)$$

$$g^{0.5}(\text{CH}) = 2.29 \times M_w^{-0.08} \quad (8b)$$

$$h(\text{CH}) = 2.31 \times M_w^{-0.08} \quad (9b)$$

The calculated values of g', $g^{0.5}$, h, and the ratio $h/g^{0.5}$ for the four fractions are given in Table III. All these data reflect the increasing contraction of the μ-networks with increasing molecular weight on different length scales. It should be noted that the classical approach by Zimm and Kilb[31] resulting in $g' = g^{1.5}$ for combs fails in case of the μ-networks, which is also known for model branched polystyrenes.[34] The slight molecular weight dependence of $g^{0.5}$ and h is essentially cancelled in the ratio $h/g^{0.5}$. The ratio $h/g^{0.5}$ is significantly higher in toluene than in cyclohexane. For comblike structures,[34] this ratio was found to be smaller in toluene than in cyclohexane, in accordance with theoretical estimates.

The consistency of our hydrodynamic measurements can be demonstrated by calculation of r_η,[35] the radius of a spherical particle causing the same intrinsic viscosity, and of the Flory–Mandelkern–Scheraga parameter, β:[7,36]

$$r_\eta = [3M_w[\eta]/(10\pi N_A)]^{1/3} \quad [\eta] \text{ in cm}^3/\text{g} \quad (10)$$

$$\beta = \Phi'^{1/3}/P' = ([\eta]M_w)^{1/3}/(6\pi r_H) \quad (11)$$

$$r_\eta/r_H = \beta/9.80 \times 10^6 \text{ mol}^{1/3} \quad (12)$$

β is known to depend just slightly on solvent quality and

is therefore more "universal" than the Flory constants Φ' and P'. This way we can compare the intrinsic viscosity data with the hydrodynamic radii obtained by QELS. We achieve

in toluene:

$$r_\eta/r_H = 1.03 \pm 0.02; \quad \beta = 10.1 \times 10^6 \text{ mol}^{1/3} \quad (13)$$

in cyclohexane:

$$r_\eta/r_H = 1.07 \pm 0.03; \quad \beta = 10.5 \times 10^6 \text{ mol}^{1/3} \quad (14)$$

The β value shows that the hydrodynamic behavior is near the hard-sphere limit ($\beta = 9.80 \times 10^6$ mol$^{1/3}$, see also the bridging relationship (eq 12)) and below the value known for Gaussian chains of $\beta = 12.87 \times 10^6$ mol$^{1/3}$ (Kirkwood, Riseman) or $\beta = 12.63 \times 10^6$ mol$^{1/3}$ (Zimm). Renormalization group theory[37] yields β values of 9.60×10^6 mol$^{1/3}$ and 11.2×10^6 mol$^{1/3}$ for Θ and good solvent conditions, respectively. In practice, the ratio r_η/r_H is rather insensitive to structural changes. For branched structures, this ratio is very close to unity, irrespective of the solvent quality,[34] and for linear chains in a good solvent values of about 1.1 are reported.[43] The present experiments yield a significantly larger r_η/r_H ratio for the Θ solvent than for the good solvent toluene, in contradiction to the theoretical expectations. No explanations for this small, but significant, discrepancy can be given (see also the discussion of $h/g^{1/2}$ above).

Theoretical considerations[38] have established that the ratio $h/g^{1/2}$ is very sensitive on the degree of branching. Our data in toluene are nearly independent of molecular weight and comply with a highly cross-linked structure. For a more practical understanding, it should be stated that h depends on $\sum(1/R_{ij})$, where R_{ij} is the distance between monomers i and j, and $g^{0.5}$ is a function of $(\sum R_{ij}^2)^{0.5}$. Therefore, h is more sensitive to changes of shorter distances, while $g^{0.5}$ reflects the contraction of monomers that are widely separated. We can conclude from our hydrodynamic measurements that the influence of the excluded volume is more pronounced on a local scale (e.g., a single chain between two cross-links) whereas the whole μ-network is just slightly expanded. On a larger scale, the excluded volume is possibly screened off.[39]

In cyclohexane we obtain a completely different situation: the ratio $h/g^{1/2}$ is also independent of the molecular weight but close to unity. Therefore we conclude that in a Θ solvent the contraction of the μ-networks in comparison to linear chains is the same on all size scales. This implies that the μ-networks have to be self-similar: the internal structure must comply with the molecular weight dependent properties. These facts and the possible existence of a certain screening length dividing the two different regimes will be tested with neutron scattering.

It should be noted that we have listed in Table II the second virial coefficient A_2 and the constants k_D and k_H characterizing the concentration dependence of the hydrodynamic radius and the intrinsic viscosity, respectively. As observed for other branched systems, the k_H values in toluene are significantly higher than for linear structures. The experimental values in cyclohexane could not be determined with a sufficient accuracy, because the data scatter too much due to the very low concentrations applied. For a more accurate determination of these constants, the concentration range of the measurements has be expanded, which will then allow a more significant comparison with theory.

2. Neutron Scattering. The neutron-scattering measurements in 2% solutions of the μ-networks in deuterated toluene and cyclohexane cannot be properly interpreted as dilute solution experiments. Therefore, no molecular data such as the radius of gyration or the absolute molecular weight can be extracted from our present experiments, which were performed to investigate how cross-linking affects the internal structure of μ-networks. This work must be complemented by future experiments in more dilute solutions, which, however, require extended neutron beam time. Possible perturbations caused by the large concentrations are a slight compression in good solvents due to the altered thermodynamic environment or some cluster formation due to the overlap of labeled species. For spherical particles we can further think of a contribution from a structur factor caused by liquidlike order. Keeping this in mind, we should concentrate on the information obtained at higher momentum transfer related with smaller distances, where the influence of concentration should be traceable.

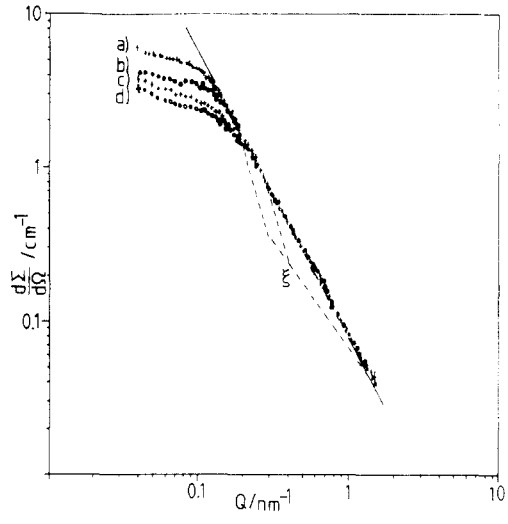

Figure 11. Small-angle neutron scattering data of the sample N4200/66 (a), N4600/104 (b), N1700/39 (c), and N1000/55 (d) in 2% toluene solution. The dashed line sketches the behavior of networks with a homogeneous mesh size distribution and a distinct correlation length ξ for two different cross-linking densities (see text).

The more compact structure seen in light-scattering experiments must influence the spatial pair correlation function of monomer units, which is directly measured as a Fourier transform by the Q dependence of the absolute scattering cross section $d\Sigma/d\Omega$ (see, for instance, ref 39). In this context we note the relation of the radial mass distribution with the molecular weight dependence of the radius of gyration, $R_G = \langle s^2 \rangle_z^{0.5}$:

$$M_\omega \sim R_G^{d_f} \quad (15)$$

Fourier transformation from R to Q space results in

$$(d\Sigma/d\Omega)(Q) \sim Q^{-d_f} \quad (16)$$

For simplicity, we have assumed a scaling approach, resulting in a simple exponential law. If the radius–mass scaling holds over several decades, d_f defines the fractal dimension of the object.

Figure 11 shows the scattering curves of the samples N4200/66, N3600/104, N1700/39, and N1000/55 in a log $d\Sigma/d\Omega$–log Q plot for good solvent conditions covering a wide range of absolute molecular weights and a factor of 2 of cross-linking densities. The scattering vector Q is defined as

$$Q = (4\pi/\lambda) \sin(\Theta/2) \quad (17)$$

where λ is the wavelength of the incoming neutrons and

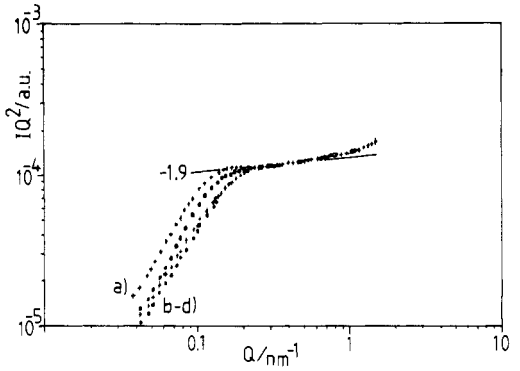

Figure 12. Kratky plot of the data described in Figure 11.

Θ the angle between the incident and scattered beam. Error bars due to statistics are as small as indicated in the figure.

We observe that all curves are running into one nearly straight line given by the same Q-dependent absolute scattering cross section, that is to say the same size-dependent local density. The spatial dimensionality given by the slope of the line is obtained as $d_f = 1.93 \pm 0.03$. Obviously this slope is independent of molecular weight and cross-linking density. The "linear" regime covers a range of distances between 3 nm and a macroscopic cutoff determined by the absolute molecular weight of the μ-network. The different molecular weights of the samples varying over more than 1 decade are not seen in the absolute scattering intensities extrapolated to $Q \rightarrow 0$. Also, the apparent radii of gyration of 6–10 nm, which can be evaluated by fitting the form factor of a Gaussian chain to the upper part of scattering profile, are too small compared with the values obtained by light scattering in high dilution. As already discussed, this is expected for the transition from a dilute to a semidilute solution.

Figure 12 shows the log IQ^2 versus log Q plot of the same data, which is more sensitive to small deviations of the exponent. Here we can observe a small, but significant, curvature to a higher exponent at lower Q values. It is not experimentally evident whether we observe scaling or nonscaling behavior. Theoretical calculations made for many-arm star polymers[40] are prognosticating a similar behavior in an intermediate regime of the scattering curve but call it "quasifractal".

The molecular weight independence of the slope proves the self-similarity hypothesis. More suprising is the independence upon cross-linking density, which cannot be explained in a straightforward way. The two dashed lines in Figure 11 indicate the expected behavior for entangled networks in good solvents:[39] below a screening length ξ (or inside of a "blob") we expect an excluded volume behavior with a slope of −1.66, above this value the scattering experiment has to reflect the three-dimensional nature of the network. ξ must scale with the molecular weight of the polymer chain between two cross-links. Clearly, this "ideal" behavior is not observed. Discussing our data within the same picture, we have a continuum of screening lengths which should be independent of cross-linking density. Comparing the averaged exponent d_f of SANS, $d_f \pm 1.9$, with the calculated exponent obtained by light scattering from the molecular weight dependence of the radius of gyration, d_f(calcd) = 1/0.47 = 2.13 (c.f. eq 6a and 13), we find that in toluene the μ-networks are really more swollen on a local scale (SANS) whereas the influence of excluded volume is decreased on the scale detected by light scattering. This is in good agreement with the hydrodynamic measurements of the previous chapter. Further

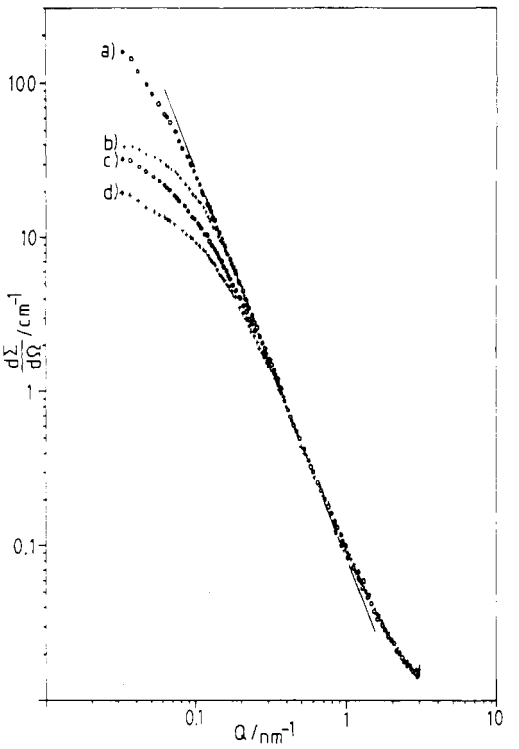

Figure 13. SANS data of the samples (a–d, see Figure 11) in 2% cyclohexane solutions.

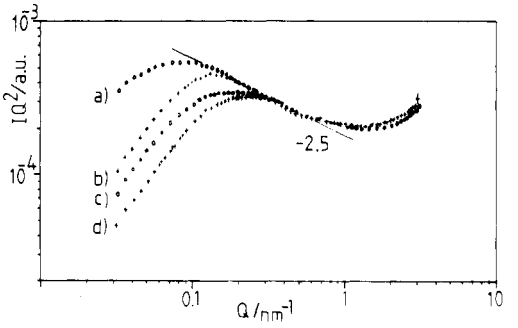

Figure 14. Kratky plot of the cyclohexane data.

SANS experiments with larger μ-networks in more dilute solution have to be carried out in order to observe the transition between the different scattering regimes and to describe the size-dependent influence of a good solvent in a completed way.

Figures 13 and 14 represent the scattering curves of the same polymers in cyclohexane at 34.5 °C, which is the Θ temperature of linear polystyrene. It is well-known[10] that a lower Θ temperature should be expected for branched or cyclic structures, but we have no exact values for our samples. The A_2 values determined with light scattering are close to zero. One should also note that even in cyclohexane we do not reach with neutron-scattering experiments the dilute regime where we can observe the unperturbed scattering of a single molecule, although the μ-networks are less extended than in toluene solution. This is possibly due to the vanishing repulsive forces between different μ-networks and cluster formation.

The curvature in the center region of Figure 14 is larger than in Figure 11. By approximating these results with a limiting exponent, we get $d_f' = 2.52 \pm 0.04$. At large Q values we probably observe the influence of chain stiffness, which causes a decrease in the slope for distances smaller than ~2 nm. The comparison of the exponent d_f' with the calculated value from light-scattering data (d_f'(calcd) =

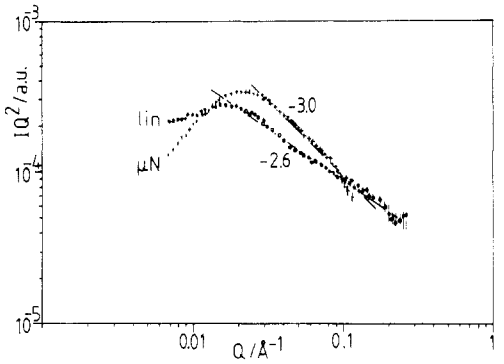

Figure 15. Kratky plot of SANS bulk experiments of sample N1600/25 in a linear (Lin1700) and cross-linked (N800/24) environment.

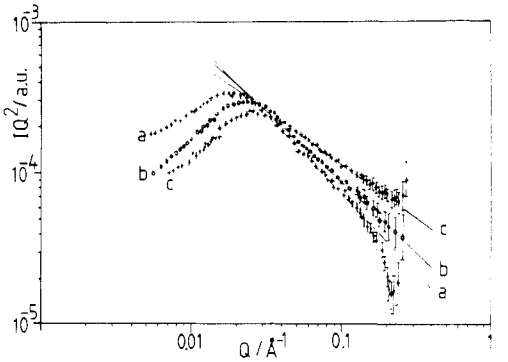

Figure 16. Kratky plot of the molecular weight dependence of the scattering function in cross-linked environments: (a) N2300/62, (b) N1700/62, and (c) N1300/62.

2.38) leads to a satisfactory agreement; even small changes in the exponent of eq 6b would result in a better correspondence. As already indicated by the equality of the contraction factors, the μ-networks seem to be self-similar in the unperturbed state.

Concluding the discussion of the solution data, it should be said that a theoretical calculation made for fractal networks[40] results in scaling exponents for the spatial pair correlation function of −2.0 and −2.5 (Θ solvent and good solvent, respectively), which are not too far away from our results. We cannot distinguish accurately enough between a "scaling" or "nonscaling" behavior due to the limited resolution of our experiments. However, a description of the here examined μ-networks with a scaling approach works and leads also to a fair agreement with theory.

The examination of the μ-networks in the bulk state is essential for the understanding of the dynamic mechanical experiments carried out in a melt of pure μ-network material. These experiments will be described in the subsequent paper.[9] We have to use different samples than the ones characterized with SANS in solution because we wish to measure deuterated probe μ-networks in protonated environments in order to minimize the influence of void scattering. This change should not give rise to any difficulties because of the independence shown upon cross-linking density and molecular weight of the scattering profiles in toluene and cyclohexane solutions.

A polymer in a linear polymer environment of the same type should behave as in a Θ solvent. However, in μ-networks there are topological restrictions which should hinder the molecule to maintain the unperturbed state; a linear chain cannot penetrate into all "holes" that are within reach of small solvent molecules. This effect should be increased for μ-network particles in an environment of the same type. The topological restrictions that counteract the penetration of different coils are larger.

Figure 15 represents neutron-scattering curves of the sample N1600/25 in a linear and μ-network matrix of the same cross-linking density (Lin1700 and N800/24, respectively) in a log IQ^2 versus log Q plot. In comparison with our measurements in cyclohexane (Figure 13), we observe a further increase of compression: the description with a simple exponential law in the center region is more accurate and results in a slope of −2.62 in the linear environment and of −3.0 in the μ-network material. Therefore, we conclude that the μ-networks are still interpenetrated by the linear chains, although the local monomer density is higher than in low molecular weight Θ solvents. The difference of 0.1 in the scaling exponent is a minor effect in comparison with the strong increase of 0.5 for the μ-network environment. Here, the molecules behave nearly like massive spheres of constant density. It is, however, worth mentioning that we have not yet reached the limit where the scattering behavior is determined by the inner surface, given by $d\Sigma/d\Omega(Q) \sim Q^{-4}$, in the intermediate scattering regime.[41]

For bulk experiments, the influence of the persistence length vanishes in the limit of large Q values. In some cases we can observe the scaling behavior of the center part of the scattering profile down to the first Bragg peaks of monomer units. Taking into account the strong geometrical restrictions in such a melt, this fact can be explained by assuming that each part of the polymer must fit into one of a small number of possible configurations, and thus the energetical differences between cis and trans becomes a weak contribution to the total free energy. Calling the Θ state unperturbed, we should name this situation "compressed".

An important test of this assumption is the examination of the molecular weight dependence down to lower molecular weights. Even when the chains are strongly compressed, the surface of the structure must be drained with other chains. The lower the molecular weight the higher is the probability that some segment belonging to the matrix μ-network particles is within the probe structure. This shown in Figure 16, where three fractions from the same cross-linking reaction (N2300/62–N1000/62, equal chain lengths between cross-links) have been examined in a cross-linked environment (N2900/71), the apparent molecular weights M_w(app) being between 120 000 and 330 000 g/mol. We observe that the width of the scaling regime decreases with decreasing molecular weight. Furthermore, the scaling exponent (within all uncertainties) is changed from −3.0 to −2.92 and −2.70, respectively. A similar behavior was observed for the series N770/25–N1600/25 and N800/37–N1600/37.[42] Here, the decreases of the scaling exponents are less pronounced because of the higher cross-linking densities, thus supporting the interpretation of the decrease as caused by interpenetration at the surface of the μ-networks.

In the SANS bulk experiments, we also cannot definitely decide whether a scaling or nonscaling description is more appropriate, although indications of scaling are more pronounced than for the solution data. This can be impressively demonstrated by the log $d\Sigma/d\Omega$–log Q plots for the samples N1600/25 (linear matrix Lin1700) and N2300/62 (μ-network matrix N2900/71), where we observe a "linear" behavior over more than 3 decades of the scattering cross section, see Figure 17. This is possibly due to the above-mentioned apparent suppression of the persistence length, which would allow the development of a "fractal" structure even at sizes comparable to the elementary chain units of the network. However, one should not overemphasize this possibility of a scaling description;

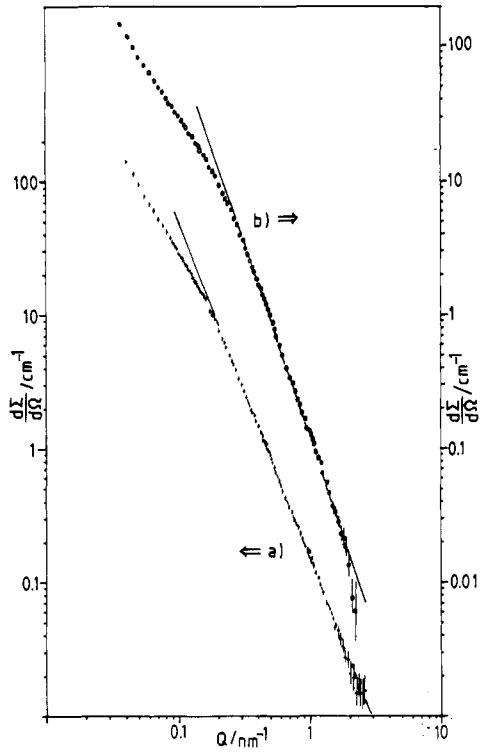

Figure 17. Absolute scattering cross section of N1600/25 in a linear matrix (a) and N230062 in a μ-network matrix (b).

it simplifies the mathematical treatment but does not alter the physical meaning of the measurements.

V. Conclusions

μ-Network systems obtained by condensation of telechelic chains in solution below a critical volume fraction of polymer, Φ_P(crit), can easily be fractionated, and the fractions can be characterized by GPC, solution viscosimetry, static and dynamic light scattering, and small-angle neutron scattering. Thus, the well-established methods of analyzing the structure of linear and branched macromolecules in solution can be applied to network analysis. Quantitative measurements of the contraction factors g', $g^{0.5}$, and h of the μ-networks compared to linear chains in toluene (good solvent) and cyclohexane (Θ solvent) can be evaluated and result in three different facts: (1) μ-Networks represent more dense structures than linear chains, as expected. The local monomer density is increased up to a factor of 6. The Flory–Mandelkern–Scherage parameter is close to that of an undrained sphere. (2) In a Θ solvent, the μ-networks are self-similar. With a Gaussian chain as a reference, the contraction is seen on all length scales the same way. (3) This is not the fact in a good solvent. Hydrodynamic measurements suggest that the influence of excluded volume is more pronounced on a local scale than on the overall dimensions. This is known as "screening" in the case of entangled polymer systems. Possible polydispersity effects will be analyzed further when the one-line analysis of GPC elution curves by static and dynamic light scattering becomes available to us.

With SANS experiments, one can confirm the observations made with light scattering. The Q-dependent scattering cross section, which is the Fourier transform of the radial density function, can be compared with the scaling of the radius of gyration on molecular weight. For a good solvent the density on a local scale seen by the neutrons is remarkably lower; the two scalings of LS and SANS do not correspond. No distinct screening length but a broad distribution can be determined. The transition to the "macroscopic" scattering behavior in the low-Q range could not be analyzed in our present SANS experiments, performed at only one polymer concentration of 2%.

In cyclohexane, the data agree within the experimental accuracy: the exponent of $S(Q) \sim Q^{-2.5}$ corresponds to $\langle s^2 \rangle_z^{0.5} \sim M^{0.42}$ via eq 6b. Since the cross-linking reaction occurred relatively close to a critical gel concentration, the network structure can be also analyzed in terms of a "fractal" description,[40] which is discussed to be valid near phase transitions. The exponent obtained for the radial density function, $d_f = 2.5$, is independent of the molecular weight as well as the parent chain length of the μ-networks and clearly indicates some "self-similarity". It agrees well with the calculated exponent of percolation clusters at the gel point. More specified statements concerning this special question as to the universality of this phenomenon and possible differences of the topology of μ-networks and percolation clusters have to await further experiments, which are presently being carried out. The neutron-scattering results of deuterated μ-networks in matrices of PS chains and μ-networks, respectively, demonstrate that the μ-networks can be freely interpenetrated by chains and behave nearly as in the Θ solvent. On the other hand, μ-networks become "compressed" when surrounded by other networks in the bulk state. Interpenetration becomes increasingly impeded in systems with larger μ-network sizes.

Acknowledgment. We thank T. A. Vilgis for many helpful comments and discussions. Support by the Deutsche Forschungsgemeinschaft is gratefully acknowledged.

Registry No. PS, 9003-53-6; bis(dichloromethylsilyl)ethane, 3353-69-3; neutron, 12586-31-1.

References and Notes

(1) Rempp, P.; Herz, J.; Borchard, W. *Adv. Polym. Sci.* **1978**, *26*, 105.
(2) Valles, E. V.; Macosko, C. W. *Macromolecules* **1979**, *12*, 673.
(3) Havranek, A.; Nedbal, J.; Berick, C.; Ilawski, M.; Dusek, K. *Polym. Bull. (Berlin)* **1980**, *3*, 497.
(4) Weiss, P.; Hild, G.; Herz, J.; Rempp, P. *Makromol. Chem.* **1970**, *135*, 249.
(5) Mark, J. E. *Adv. Polym. Sci.* **1982**, *44*, 1.
(6) Mark, J. E.; Quesnel, J. P. *Adv. Polym. Sci.* **1984**, *65*, 135.
(7) Flory, J. P. *Principles of Polymer Chemistry*; Cornell University Press: Ithaca, NY, 1953.
(8) Antonietti, M.; Sillescu, H.; Schmidt, M.; Schuch, H. *Macromolecules* **1988**, *21*, 736.
(9) Antonietti, M.; Fölsch, K. J.; Pakula, T.; Sillescu, H. *Macromolecules*, following paper in this issue.
(10) Roover, J.; Toporowski, P. M. *Macromolecules* **1983**, *16*, 843.
(11) McKenna, G. B.; Hadziiouannou, G.; Lutz, P.; Hild, G.; Strazielle, C.; Straupe, C.; Rempp, P.; Kovacs, A. J. *Macromolecules* **1987**, *20*, 498.
(12) Gordon, M. *Proc. R. Soc. London, A* **1962**, *A268*, 240.
(13) Balaban, A. T., Ed. *Chemical Applications of Graph Theory*; Academice Press: London, New York, San Francisco, 1976.
(14) Ziabicki, A. *Polymer* **1979**, *20*, 1324.
(15) Eichinger, B. E. *Macromolecules* **1972**, *5*, 497.
(16) Burchard, W. *Adv. Polym. Sci.* **1983**, *48*, 1.
(17) Stepto, R. F. T. *Polymer* **1979**, *20*, 1324.
(18) Roovers, J.; Bywater, S. *Macromolecules* **1972**, *5*, 385.
(19) Szwarc, M. *Nature* **1956**, *178*, 1168.
(20) Cowie, J. M. G.; Worsfold, D. J.; Bywater, S. *Trans. Faraday Soc.* **1961**, *57*, 705.
(21) Antonietti, M.; Fölsch, K. J. *Makromol. Chem., Rapid Commun.* **1988**, *9*, 423.
(22) Brooks, L. *J. Am. Chem. Soc.* **1944**, *66*, 1295.
(23) Bantle, S.; Schmidt, M.; Burchard, W. *Macromolecules* **1982**, *15*, 1604.
(24) Neutron Research Facilities at the ILL High Flux Reactor, ILL, Grenoble, June 1986.
(25) Antonietti, M.; Countandin, J.; Sillescu, H. *Macromolecules* **1986**, *19*, 793.
(26) Outer, P.; Carr, C. I.; Zimm, B. H. *J. Chem. Phys.* **1950**, *18*, 830.
(27) Appelt, B.; Meyerhoff, G. *Macromolecules* **1980**, *13*, 657.

(28) Brandup, H.; Immergut, E. H. Eds. *Polymer Handbook*; Wiley: New York, 1974.
(29) Schmidt, M.; Burchard, W. *Macromolecules* **1981**, *14*, 210.
(30) Bremser, W. Diplomarbeit, Mainz, 1988.
(31) Zimm, B. H.; Kilb, R. W. *J. Polym. Sci.* **1959**, *37*, 19.
(32) Kurata, M.; Abe, M.; Iwana, M.; Matsushima, M. *Polym. J. (Tokyo)* **1972**, *3*, 729.
(33) Zimm, B. H.; Stockmayer, W. *J. Chem. Phys.* **1949**, *17*, 1301.
(34) Roovers, J.; Toporowski, M. *J. Polym. Sci., Polym. Phys. Ed.* **1980**, *18*, 1907.
(35) Yamakawa, H. *Modern Theory of Polymer Solutions*; Harper & Row: New York, 1971.
(36) Scherage, H. A.; Mandelkern, L. *J. Am. Chem. Soc.* **1953**, *75*, 179.
(37) Oono, Y.; Kohmoto, M. *J. Chem. Phys.* **1983**, *78*, 520; *J. Chem. Phys.* **1983**, *79*, 4629.
(38) Berry, G. C. *J. Polym. Sci., Polym. Phys. Ed.* **1968**, *6*, 1551.
(39) de Gennes, P. G. *Scaling Concepts in Polymer Science*; Cornell University Press: Ithaca, NY, 1979.
(40) Vilgis, T. A. *Phys. Rev. A* **1987**, *36*(3), 1506.
(41) Porod, G. *Kolloid Z.* **1951**, *124*, 83.
(42) Fölsch, K. J. Dissertation, Mainz, 1988.
(43) McDonnell, M. E.; Jamieson, A. M. *J. Polym. Sci.* **1980**, *18*, 1781.

Micronetworks by End-Linking of Polystyrene. 2. Dynamic Mechanical Behavior and Diffusion Experiments in the Bulk

Markus Antonietti, Karl J. Fölsch, and Hans Sillescu*

Institut für Physikalische Chemie der Universität Mainz, Jakob Welder Weg 15, D-6500 Mainz, West Germany

Tadeusz Pakula

Max Planck Institut für Polymerforschung Mainz, Jakob Welder Weg 13, D-6500 Mainz, West Germany. *Received August 2, 1988; Revised Manuscript Received November 12, 1988*

ABSTRACT: The frequency-dependent storage and loss moduli, $G'(\omega)$ and $G''(\omega)$, have been determined for polystyrene μ-networks (see preceding paper). By application of the temperature–frequency shift procedure we have obtained spectra within a frequency range of ω between 10^{-3} and 10^{3} s^{-1}. In all cases, power laws $G'(\omega) \sim G''(\omega) \sim \omega^{\alpha}$ were found to apply over 5 decades in frequency. α increases from 0.2 to 0.5 as the number of monomers between cross-links, P_c, is decreased from 141 to 23. The absolute values of $G'(\omega)$ and $G''(\omega)$ decrease with decreasing P_c, both being below the moduli values of entangled linear PS. $\tan \delta = G''/G'$ increases in the same order and approaches unity at $P_c = 23$. By a dilution experiment we can suggest a division of this behavior in two contributions: a part characterized by $G'(\omega) = G''(\omega) \sim \omega^{0.5}$ describes the internal dynamics of the μ-networks whereas the remainder is given by a P_c-dependent chain–chain interaction with a scalable lifetime distribution. The results are in harmony with similar findings in comb-shaped polymers and networks obtained by cross-linking of telechelic chains at the gel point. These data also support the description of μ-networks as "fractal" structures, which was raised during the structure examinations. Although more detailed experiments are necessary, the problems concerning this description are discussed. The tracer diffusion of labeled PS chains in μ-networks is not different from that in matrices of entangled linear PS. This result cannot be understood within a tube model having cross-links as fixed obstacles but requires consideration of the internal μ-network dynamics.

I. Introduction

In our previous paper,[1] the preceding paper in this issue, we have described the synthesis of model μ-networks and their characterization with light and neutron scattering, gel permeation chromatography, and viscosimetric measurements. We have demonstrated that we can approximate the local structure of these particles by a "fractal" distribution of the local monomer density. The scaling laws of diverse properties comply with measurements on other differently branched structures (references cited in ref 1).

The subject of this publication is the description of the dynamic behavior of these structures in the bulk state above the glass transition temperature. We present results of two different techniques: dynamic shear experiments determine the viscoelastic properties of these molecules, thus resulting in spectra of relaxation times which can be related to the molecular architecture (c.f. ref 2). In addition, diffusion experiments of linear probe chains reflect the local structure of entanglements and cross-links of the μ-network environment.[3,4] The combination of the results of these two techniques and the structure data of ref 1 should lead to a general picture for the dynamics of a whole class of cross-linked structures. Furthermore, we discuss whether the description of polymer networks as fractal structures, which was successfully used at the gel point of networks cross-linked in the bulk state,[5,6] can be extended to differently cross-linked structures, at least in a limited frequency and space regime. This should also contribute to a still open discussion that was induced by neutron-scattering results on stretched networks and could not be explained by classical structure assumptions.[7]

II. Experimental Section

1. **Dynamic Mechanical Experiments.** The μ-network samples were precipitated from solution and carefully dried overnight in vacuo at 80 °C. By compression molding at 150 °C optically clear disks with 13-mm diameter were prepared, fitting the geometry of a plate/plate rheometer. A Rheometrics RMS 800 apparatus was used in an oscillating low-amplitude mode in a frequency range between 10^{-2} and 10^{2} rad·s^{-1} with an amplitude of 2%. For one chosen sample it was checked that our measurements are within the linear regime, which typically goes up to 20% strain. The measurements were controlled by a FRT2000 frequency response analyzer, which also records the complex torque. A stream of dry nitrogen was blown over the sample in order to avoid thermal oxidative damage during the measurements performed at 130–210 °C. After the sample was heated to the maximum temperature, the measurements at 150 °C were repeated in order to check for alteration. The changes remain within

0024-9297/89/2222-2812$01.50/0